NF_3: UV absorption spectrum temperature dependence and the atmospheric and climate forcing implications

Vassileios C. Papadimitriou,[1,2,3] Max R. McGillen,[1,2] Eric L. Fleming,[4,5] Charles H. Jackman,[4] and James B. Burkholder[1]

Received 9 November 2012; revised 18 December 2012; accepted 24 December 2012; published 30 January 2013.

[1] Nitrogen trifluoride (NF_3) is an atmospherically persistent greenhouse gas that is primarily removed by UV photolysis and reaction with $O(^1D)$ atoms. In this work, the NF_3 gas-phase UV absorption spectrum, $\sigma(\lambda,T)$, was measured at 16 wavelengths between 184.95 and 250 nm at temperatures between 212 and 296 K. A significant spectrum temperature dependence was observed in the wavelength region most relevant to atmospheric photolysis (200–220 nm) with a decrease in σ(210 nm,T) of ~45% between 296 and 212 K. Atmospheric photolysis rates and global annually averaged lifetimes of NF_3 were calculated using the Goddard Space Flight Center 2-D model and the $\sigma(\lambda,T)$ parameterization developed in this work. Including the UV absorption spectrum temperature dependence increased the stratospheric photolysis lifetime from 610 to 762 years and the total global lifetime from 484 to 585 years; the NF_3 global warming potentials on the 20-, 100-, and 500-year time horizons increased <0.3, 1.1, and 6.5% to 13,300, 17,700, and 19,700, respectively.
Citation: Papadimitriou, V. C., M. R. McGillen, E. L. Fleming, C. H. Jackman, and J. B. Burkholder (2013), NF_3: UV absorption spectrum temperature dependence and the atmospheric and climate forcing implications, *Geophys. Res. Lett.*, *40*, 440–445, doi:10.1002/grl.50120.

1. Introduction

[2] Nitrogen trifluoride (NF_3) is an atmospherically persistent potent greenhouse gas (GHG), included in the Kyoto protocol, which is used in the semiconductor and electronics industry. NF_3 is emitted into the atmosphere and removed primarily in the upper atmosphere (stratosphere and mesosphere) by photolysis and reaction with electronically excited oxygen atoms, $O(^1D)$. The atmospheric abundance of NF_3 in 2011 was 0.86 ppt, with a growth rate of ~0.1 ppt yr^{-1} between 2008 and 2011 [*Arnold et al.*, 2012].

[3] The atmospheric lifetime of NF_3 has been evaluated in several recent studies to be ~500 years [*Prather and Hsu*, 2008; *Zhao et al.*, 2010; *Dillon et al.*, 2011; *WMO*, 2011], with short-wavelength UV photolysis being its predominant atmospheric loss process. The 500-year time horizon global warming potential (GWP) of NF_3 is estimated to be 18,500 [*WMO*, 2011], which is comparable with that of SF_6, making NF_3 one of the most potent GHG in the atmosphere. NF_3 is, therefore, considered a persistent climate-forcing agent with an impact extending over the next millennium. Understanding the environmental impact of NF_3 requires a thorough understanding of not only its usage and emissions but also its atmospheric loss processes to better define its atmospheric lifetime, τ, and, thus, its contribution to climate forcing. To the best of our knowledge, the NF_3 UV absorption spectrum temperature dependence has been neglected in all previous atmospheric lifetime calculations due to a lack of experimental data. A decrease in the NF_3 absorption spectrum, $\sigma(\lambda,T)$, at the temperatures relevant to the stratosphere, where NF_3 is primarily removed, would lead to even longer calculated lifetimes and warrants evaluation.

[4] In this work, the gas-phase UV absorption spectrum for NF_3 was measured at 16 discrete wavelengths between 184.9 and 250 nm at temperatures between 212 and 296 K. The present results are compared with previously reported room temperature spectra [*Makeev et al.*, 1975; *Molina et al.*, 1995; *Dillon et al.*, 2010] and discrepancies are discussed. The wavelength and temperature dependence of the absorption spectrum, $\sigma(\lambda,T)$, obtained in this work was parameterized for use in atmospheric model calculations. The NASA Goddard Space Flight Center (GSFC) 2-D coupled chemistry-radiation-dynamics model [*Fleming et al.*, 2007, 2011] was used to evaluate the atmospheric photolysis, local and global annually averaged lifetimes of NF_3, and the significance of including the UV spectrum temperature dependence.

2. Experimental Details

[5] UV absorption cross-sections, $\sigma(\lambda,T)$, for NF_3 were measured at 212, 231, 253, 273, and 296 K at 16 discrete wavelengths between 184.9 and 250 nm. The experimental apparatus was similar to that used in a recent study from our laboratory [*Rontu Carlon et al.*, 2010] and is only described briefly here. The major components of the apparatus are a 30 W deuterium (D_2) or atomic lamp light sources, a jacketed absorption cell with a 90.4 cm path length, a 0.25 m monochromator with a photomultiplier tube detector, and a photodiode detector. The cell temperature was adjusted by circulating a temperature-regulated fluid through its jacket. The temperature was measured at the entrance and exit of the cell, with an accuracy of ~0.5 K for temperatures >253 K and ~1 K for the lower temperatures. The monochromator wavelength was calibrated using atomic lamps

[1]Earth System Research Laboratory, Chemical Sciences Division, National Oceanic and Atmospheric Administration, Boulder, Colorado, USA.
[2]Cooperative Institute for Research in Environmental Sciences, University of Colorado, Boulder, Colorado, USA.
[3]Laboratory of Photochemistry and Chemical Kinetics, Department of Chemistry, University of Crete, Heraklion, Crete, Greece.
[4]NASA Goddard Space Flight Center, Greenbelt, Maryland, USA.
[5]Science Systems and Applications, Inc., Lanham, Maryland, USA.

Corresponding author: James B. Burkholder, Earth System Research Laboratory, Chemical Sciences Division, National Oceanic and Atmospheric Administration, 325 Broadway, Boulder, Colorado, 80305, USA. (James.B.Burkholder@noaa.gov)

0094-8276/13/10.1002/grl.50120

to ±0.1 nm and its resolution was ~1 nm (full width at half maximum). For measurements at wavelengths <220 nm, a 193 nm dielectric mirror was used to direct the light source onto the entrance slit of the monochromator to minimize scattered light detection. A 280 nm long-pass filter was inserted into the beam path to record background signals.

[6] Absorption cross-sections were determined using Beer's law:

$$A(\lambda) = -\ln[I(\lambda)/I_0(\lambda)] = \sigma(\lambda, T) \times L \times [NF_3], \quad (1)$$

where A is the absorbance at wavelength λ; $I(\lambda)$ and $I_0(\lambda)$ are the measured light intensity with and without the sample present in the absorption cell, respectively; L is the absorption path length (90.4 ± 0.3 cm); and $[NF_3]$ is the concentration of NF_3. NF_3 concentrations were determined using absolute pressure measurements and the ideal gas law. Absorbance was measured for a range of concentrations and σ(λ,T) determined from a linear least-squares fit of A versus $[NF_3]$.

[7] Measurements were performed by first flushing the absorption cell with He bath gas, evacuating the cell, and then recording $I_0(\lambda)$. The cell was then flushed with NF_3, filled to a known pressure, and $I(\lambda)$ was measured. The absorption cell was then evacuated and refilled to a different NF_3 concentration, and $I(\lambda)$ was recorded. This procedure was repeated at least eight times to obtain $A(\lambda)$ values in the range 0.02 and 0.5; at the longer wavelengths, the range in $A(\lambda)$ values was less.

[8] σ(λ,T) was also measured, in several experiments, using neutral density filters (OD: 0.2–0.8) in the optical path between the light source and the absorption cell to test for possible NF_3 photolysis, as well as the linearity of the detection system. The σ(λ,T) values measured with and without the filters agreed to better than 1%, that is, within the precision of the measurements.

[9] Measurements of σ(λ,T) at the 184.95 nm atomic Hg line were made using an Hg Pen-Ray light source and photodiode detector. The measurement procedures were identical to those described above. Band-pass filters mounted in front of the Hg lamp and detector were used to isolate the 184.95 nm Hg line and minimize exposure of the NF_3 sample to other lines from the lamp. Experiments performed without the source filter yielded identical results to within the precision of the measurements, that is, NF_3 photolysis was negligible.

[10] $I(\lambda)$, $I_0(\lambda)$, and the cell pressure were recorded at a 1 kHz sampling rate for at least ~20 s, an average value was used in the data analysis. The signals were stable to better than 0.5% and $I_0(\lambda)$ values were measured at the beginning and end of an experiment, which had a typical duration of 15 min, agreed to within 0.5%; this corresponds to an absorbance uncertainty of less than ~0.005.

[11] NF_3 (electronic grade, 99.99%) and He (ultrahigh purity, 99.999%) were used as supplied. Pure NF_3 was used in the majority of the measurements, whereas several test measurements were performed using 1.0% and 10.1% mixtures of NF_3 in He. Measurements performed with the gas mixtures yielded results in excellent agreement, to within 1% or better, with σ(λ,T) measured using pure NF_3 samples. Gas mixtures were prepared manometrically in 12 L Pyrex bulbs. N_2O (ultrahigh purity, 99.997%) used in several test measurements was degased during mixture preparation via freeze-pump-thaw cycles. N_2O in He mixtures, 0.1% and 1.0%, were used in the short-wavelength (185–210 nm) measurements, whereas pure N_2O was used for measurements in the 215–230 nm range. Pressures were measured using 100 and 1000 Torr capacitance manometers (±0.2%).

3. Results and Discussion

[12] Gas-phase UV absorption cross-sections, σ(λ,T), for NF_3 were determined at 16 discrete wavelengths over the range 184.95–250 nm at 212, 231, 253, 273, and 296 K. The results are summarized in Table S1 in the Supplementary Material and plotted in Figure 1. The σ(λ,T) values are averages of all the measurements performed over a range of conditions at each wavelength. Measurements were performed under different experimental conditions, including variations in the range of absorbance, lamp intensity, as well as using pure and mixtures of NF_3 in He. In all cases, the measured absorption signals varied linearly with $[NF_3]$ at all wavelengths, that is, obeyed Beer's law. In most cases, three to four sets of measurements were performed at each wavelength and temperature. The precision of the measurements was high, particularly in the wavelength range most relevant for atmospheric photolysis (200–220 nm), whereas the uncertainty increased slightly at the longer wavelengths due primarily to the weaker NF_3 absorption signals. The data reproducibility was tested extensively, including variations of the optical setup; different optical filtering, lamp intensity, and monochromator resolution. The measured σ(λ,T) values under these conditions agreed to within the measurement precision. In addition, the experimental methods were further validated via measurements of the well-established N_2O absorption spectrum at room temperature at wavelengths between 185 and 230 nm. These test measurements used a similar range of pressures and the same procedures used in the NF_3 measurements. The results for N_2O were found to be in excellent agreement, to within 1% or better, with the

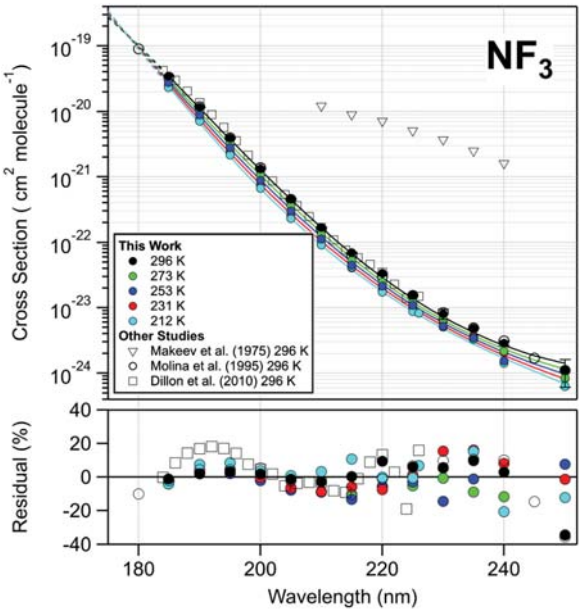

Figure 1. NF_3 UV spectrum. (top) Data measured in this work and other studies (see legend). The lines are calculated using the parameterization given in Table 2. Dashed lines are an extrapolation. (bottom) Residual of the experimentally measured cross-section data. Residual (%) = 100 × (Exp - Par) / Par.

values recommended by *Sander et al*. [2011] and recently reported from this laboratory [*Rontu Carlon et al*., 2010].

[13] The 2σ uncertainties reported in Table S1 are from the measurement precision and encompass the extremes from all of the measurements. The overall 2σ uncertainty in σ(λ,T) including estimated systematic errors was ~6% for wavelengths <205 nm, ~8% between 205 and 225 nm, and 10–15% at wavelengths >225 nm.

[14] The NF_3 spectrum decreases monotonically between 185 and 250 nm, whereas the spectrum maximum is at a wavelength shorter than included in the present work. The majority of the spectrum in this region is most likely due to a $\sigma^* \leftarrow \sigma$ electronic transition. The spectrum also shows a long-wavelength tail (Figure 1); this is also observed in the spectrum reported previously by *Molina et al*. [1995]. σ(λ,T) measurements at wavelengths >250 nm were attempted in this work and indicated further leveling off of the NF_3 spectrum at longer wavelengths. However, the precision of the measurements was low, approximately >25%, and the σ(λ,T) values are not reported here. The long-wavelength behavior may imply the presence of a weaker electronic transition(s) with a peak near 235 nm, which may correspond to a $\pi^* \leftarrow$ n or $\sigma^* \leftarrow$ n electronic transition.

[15] The NF_3 spectrum was found to have a strong dependence on temperature, particularly in the 200–220 nm wavelength region. A decrease in σ(λ,T) with decreasing temperature was observed at all wavelengths included in this study, for example, the change in σ(210 nm,T) between 296 and 212 K is ~45%. The temperature-dependent cross-section data are included in Figure 1. The tail in the long-wavelength portion of the spectrum was observed in the lower temperature spectra as well and was even more pronounced. The observed decrease in absorption cross-section in the "tail" of a continuous absorption spectrum with decreasing temperature has been observed for numerous other molecules and is qualitatively consistent with changes in the ground state Boltzmann distribution with temperature.

3.1. Comparison With Previous Studies

[16] There are three studies of the NF_3 UV absorption spectrum (all performed at room temperature) published before the present work [*Makeev et al*., 1975; *Molina et al*., 1995; *Dillon et al*., 2010]. The spectra are included in Figure 1 for comparison with the results from this work. The spectrum reported by *Makeev et al*. [1975] seems to be subject to measurement error and is not considered further. The present results are consistent with the UV absorption spectrum reported by *Molina et al*., agreeing to better than 10% over the common wavelength range of 185–250 nm. In the wavelength range most critical for atmospheric photolysis (200–220 nm), the agreement is better than 5%.

[17] The spectrum reported by *Dillon et al*. [2010] is also in agreement with the present work over the atmospherically important wavelength range, agreeing to within 5–10%. At shorter and longer wavelengths, the *Dillon et al*. spectrum is systematically greater than our results by as much as ~20%. The reason for the discrepancies of the *Dillon et al*. results with the present results and those of *Molina et al*. is unknown. *Dillon et al*. corrected their cross-section measurements for the presence of an NO sample impurity on the order of ~10 ppm. The NO spectrum has discrete band structure and a 10 ppm impurity would contribute ~5% and ~50% to the measured absorbance at 215 and 226 nm, respectively. However, the differences between the spectra reported by *Dillon et al*. and in this work cannot be explained by the presence of an NO impurity alone. Based on our σ(λ,T) measurements at 225 and 226 nm, on and off a NO absorption peak, we established an upper limit to the NO impurity in our NF_3 sample of ~1 ppm. A 1 ppm NO impurity would lead to a ~2.5% overestimate in σ(225 nm,296 K) for NF_3 and significantly less error at shorter wavelengths. Therefore, an NO impurity was found not to be a significant source of systematic error in our measurements.

3.2. NF_3 Spectrum Parameterization

[18] The NF_3 absorption spectra reported in this work reduces the overall uncertainty in the wavelength region most critically relevant to atmospheric photolysis and provides the data needed for model calculations of atmospheric photolysis rates. The wavelength- and temperature-dependent UV absorption cross-sections for NF_3 were parameterized using the empirical formula given in Table 1. The fit parameters are given in Table 1 and calculated spectra are included in Figure 1 for comparison with the experimental data. The parameterization was optimized to reproduce the experimental data in the critical 200–220 nm region (Figure 1, bottom), with somewhat larger deviations obtained at the longer wavelengths. The parameterization is valid over the range of the experimental data, whereas extrapolation to lower temperatures yields reasonable σ(λ,T) values. Using the parameterization to extrapolate to longer or shorter wavelengths than included in the experiment data may be less reliable.

4. Atmospheric Implications

[19] In this section, the GSFC 2-D model was used to quantify the atmospheric loss processes of NF_3 (photolysis and $O(^1D)$ reaction) and calculate its local and global annually averaged lifetimes for present-day conditions. Steady-state calculations were performed with and without the temperature dependence of the UV absorption spectrum determined in this work to evaluate its overall significance. The possible range (uncertainty) in the calculated lifetime was evaluated using the 2σ max/min in the model kinetic and photochemical input parameters. The model results are used to report revised GWPs for NF_3 and also provide a realistic estimate in the range of possible lifetime values.

[20] Tropospheric loss processes for NF_3, for example, reaction with the OH radical [*Dillon et al*., 2011] and wet and dry deposition, are expected to be negligible and were not included in our 2-D model calculations. The contributions of various wavelength regions to the overall photolysis of NF_3 were evaluated by breaking its spectrum into four

Table 1. Absorption Cross-section, σ(λ,T), Parameterization for NF_3 (See Text)

$$\log_{10}(\sigma(\lambda,\mathrm{T})) = \sum_i A_i\lambda^i + (296-\mathrm{T})\sum_i B_i\lambda^i$$

i	A_i	B_i
0	−218.67	0.9261
1	4.03743	−0.0130187
2	−0.0295605	6.096×10^{-5}
3	9.596×10^{-5}	-9.75×10^{-8}
4	-1.3171×10^{-7}	9.76×10^{-12}
5	4.929×10^{-11}	—

wavelength regions: Lyman-α (121.567 nm), 169–190 nm, 190–230 nm, and 230–286 nm. *Dillon et al.* [2010, 2011] reported a unit photolysis quantum yield for NF_3 at 193 nm and evidence for NF_3 dissociation at 248 nm. Our model calculations assume a unit quantum for NF_3 in the VUV and UV wavelength regions at all temperatures and pressures; a quantum yield less than unity would result in longer photolytic lifetimes and greater GWPs than reported in this work. Presently, there are no experimental measurements of the NF_3 Lyman-α cross-section available in the literature. A Lyman-α cross-section of 4.8×10^{-18} cm^2 $molecule^{-1}$ was used in our model calculations, which was obtained from an extrapolation of the NF_3 VUV spectrum reported by *La Paglia and Duncan* [1961] between 126.6 and 178.6 nm. For the 169–185 nm region where no experimental data are available, an extrapolation of the parameterization given in Table 1 was used. For the longer UV wavelengths, the σ(λ,T) parameterization from the present work was used.

[21] The $O(^1D) + NF_3$ reaction is an important stratospheric loss process for NF_3. The total rate coefficient for this reaction, that is, $O(^1D)$ loss, as well as the reactive rate coefficient, NF_3 loss, for this reaction has been reported in several studies [*Sorokin et al.*, 1998; *Zhao et al.*, 2010; *Dillon et al.*, 2011], including recent work from this laboratory [*Baasandorj et al.*, 2012]. *Sander et al.* [2011] recommend the total rate coefficient value from the *Zhao et al.* study (2.4×10^{-11} cm^3 $molecule^{-1}$ s^{-1}). The more recent values from the *Dillon et al.* and *Baasandorj et al.* studies are 16% less and 6% greater than this value, respectively. More importantly for NF_3 atmospheric lifetime calculations, however, is the reactive rate coefficient, which leads to the loss of NF_3. *Zhao et al.* reported an $O(^1D)$ quenching yield for this reaction, which translates into a reactive branching ratio of between 0.95 and 1.0, that is, the reaction is mostly reactive. The *Baasandorj et al.* study used a relative rate technique to measure a reactive rate coefficient of $(2.21 \pm 0.33) \times 10^{-11}$ cm^3 $molecule^{-1}$ s^{-1}; this corresponds to a reactive branching ratio of 0.87 ± 0.13 (2σ uncertainty) based on the total rate coefficient measured in their study. The 2-D model used the Arrhenius total rate coefficient expression $k(T) = 2.0 \times 10^{-11} \exp(44/T)$ cm^3 $molecule^{-1}$ s^{-1} and a temperature-independent reactive branching ratio of $0.93 + 0.07 / -0.21$.

[22] The global annually averaged vertical profiles for the photolysis and $O(^1D)$ reactive loss terms are shown in Figure 2. Tropospheric loss is negligible. Photolytic loss, in all wavelength regions, was reduced when the absorption spectrum temperature dependence was included in the model calculation. Photolysis in the 190–230 nm region is important throughout the upper troposphere and stratosphere with >95% of the photolysis occuring at wavelengths between 200 and 220 nm. Therefore, the present measurements cover the most important UV wavelengths. The next most important wavelength region is 169–190 nm, which is ~1% of the total loss at 30 km, but makes a nearly equal contribution to the 190–230 region near 60 km. In this wavelength region, >90% of the photolysis occurs at wavelengths >180 nm and >80% occurs at wavelengths >185 nm. The 230–286 nm region makes a negligible contribution to the total photolysis throughout the entire atmosphere. Photolysis at Lyman-α becomes important above ~60 km and is the dominant loss process at altitudes >65 km. $O(^1D)$ reactive loss contributes

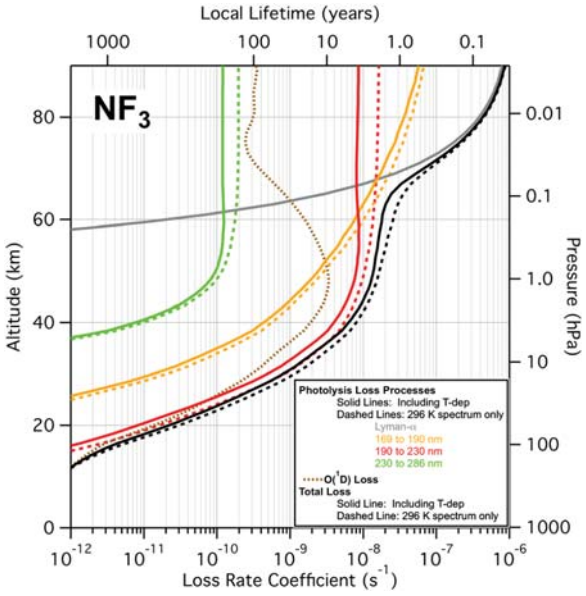

Figure 2. GSFC 2-D model global annually averaged atmospheric vertical profile results (see legend). The model results are from steady-state simulations for the present-day conditions.

significantly to NF_3 loss throughout the stratosphere. The fractional contributions of the various loss processes are given in Table 2. Photolysis is the dominant loss process and accounts for >70% of the NF_3 loss. Given the decrease in cross-section at the colder temperatures of the stratosphere, including the spectrum temperature dependence decreases the relative importance of photolysis by ~10%.

[23] The NF_3 mixing ratio and molecular loss rate vertical profiles are shown in Figure 3, assuming a surface mixing ratio boundary condition of 1 pptv for present-day conditions [*Arnold et al.*, 2012]. The maximum molecular loss rate occurs at 38.5 km, which is ~1 km higher than the maximum calculated using only the room temperature absorption spectrum. Other differences in the loss rate vertical profile with and without taking into account the UV spectrum temperature dependence are also evident in Figure 3. The calculated tropospheric, stratospheric, mesospheric, and total global annually averaged lifetimes with and without the UV spectrum temperature dependence included are given in Table 2. The total lifetime using only the room temperature spectrum was calculated to be 484 years and is comparable with the 500-year lifetime cited in *WMO* [2011]. Lyman-α photolysis, which was shown here to account for ~5% of the atmospheric loss of NF_3, was not included in the previous lifetime calculations. Including the temperature dependence of the NF_3 UV absorption spectrum in the calculation leads to a longer atmospheric lifetime of 585 years, an increase of ~20%. That is, including the UV spectrum temperature dependence had a significant effect on the global annually averaged lifetime of NF_3.

[24] Based on the estimated 2σ uncertainties of the model input kinetic and photolysis parameters, the range in the total NF_3 lifetime was determined to be 500–712 years (Table 2). The uncertainty factors for the $O(^1D)$ reaction were taken from *Sander et al.* [2011] where the 2σ uncertainty in k (298 K) was 44%. The 2σ uncertainty in the estimated

Table 2. 2-D Atmospheric Model Results of the Loss Processes for NF_3 and the Global Annually Averaged Lifetimes

	Fractional Contribution to Loss					
Model Input	121.56 nm	169–190 nm	190–230 nm	230–286 nm	Total	$O(^1D)$ Reaction
T-dep	0.063	0.100	0.549	0.002	0.713	0.287
296 K	0.044	0.096	0.634	0.002	0.776	0.224
			Lifetime (yr)			
	Trop.	Strat.	Meso.	Total	Range[a]	
T-dep	>50,000	762	2600	585	500–712	
296 K	>50,000	610	2410	484	426–563	

[a]Range of lifetime calculated using the 2σ max/min uncertainties in the kinetic and photochemical parameters (see text).

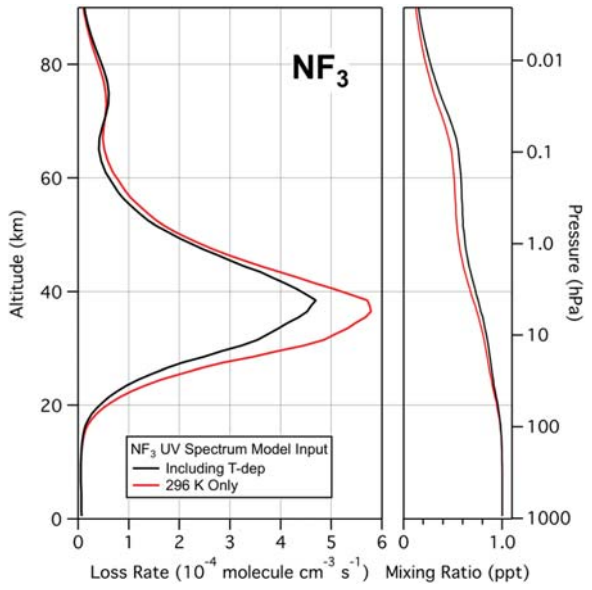

Figure 3. Steady-state GSFC 2-D global annually averaged NF_3 molecular loss rate vertical profile model results (see legend). The calculated NF_3 mixing ratio assumed a present-day surface mixing ratio boundary condition of 1 pptv.

Lyman-α cross-section was taken to be 50% and the 2σ uncertainty in the NF_3 UV absorption cross-sections was taken to be 10% for all temperatures. The obtained lifetime range, approximately ±100 years (±20%) at the 2σ level of uncertainty, reflects the current overall level of uncertainty in the NF_3 loss processes.

[25] Including the temperature dependence of the NF_3 UV absorption spectrum in the 2-D model leads to a longer atmospheric lifetime and thus greater GWPs. Scaling the GWPs reported in the *WMO* [2011] ozone assessment to the total global annually averaged NF_3 lifetime of 585 years derived in this work leads to values of 13,300, 17,700, and 19,700 on the 20, 100, and 500-year time horizons, which are <0.3, 1.1, and 6.5% greater than reported in *WMO* [2011]. The GWP uncertainty, due solely to the 2σ range in the calculated lifetime of NF_3, 500–712 years, are approximately 0.3%, 1.5%, and 7% for the 20-, 100-, and 500-year time horizons. Note that the uncertainty in the NF_3 radiative efficiency, which depends on the infrared spectrum band strengths and radiative transfer model calculations, most likely contributes a greater uncertainty to the GWP on the 100-year time horizon than the range in NF_3 lifetime.

5. Conclusions

[26] This study has provided the UV absorption spectrum data and analysis needed to critically evaluate and refine the contribution of the persistent GHG NF_3 to climate forcing. Including the temperature dependence of the UV absorption spectrum in the photolysis rate calculations, which was neglected previously, was demonstrated to have a significant impact on the calculated NF_3 atmospheric lifetime and thus estimates of its climate forcing. It was shown that stratospheric UV photolysis is the dominant atmospheric loss process for NF_3, accounting for 71% of its atmospheric loss (Table 2). Reaction with $O(^1D)$ and Lyman-α photolysis are also important loss processes that account for ~25 and ~5% of the total loss, respectively. Including the NF_3 UV spectrum temperature dependence increased its total global annually averaged lifetime by 20%. In addition, the lifetime range obtained using the 2σ estimated uncertainty in the NF_3 kinetic and photolytic parameters was determined to be 500–712 years, that is, a spread of ±20%.

[27] Atmospheric loss rate and lifetime model calculations rely on accurate laboratory kinetic and photolytic data obtained under representative atmospheric temperature and pressure conditions. Including the NF_3 UV absorption spectrum temperature dependence measured in this work and Lyman-α photolysis was shown to affect its atmospheric lifetime significantly. The modeling methods used in this work can be applied to other molecules to obtain or refine estimates of ozone depletion substance and GHG atmospheric loss processes and the associated uncertainties.

[28] **Acknowledgments.** This work was supported in part by the National Oceanic and Atmospheric Administration Climate Goal Program and the NASA Atmospheric Composition Program.

References

Arnold, T., J. Mühle, P. K. Salameh, C. M. Harth, D. J. Ivy, and R. F. Weiss (2012), Automated measurement of nitrogen trifluoride in ambient air, *Anal. Chem.*, *84*, 4798–4804.

Baasandorj, M., B. D. Hall, and J. B. Burkholder (2012), Rate coefficients for the reaction of $O(^1D)$ with the atmospherically long-lived greenhouse gases NF_3, SF_5CF_3, CHF_3, C_2F_6, c-C_4F_8, n-C_5F_{12}, and n-C_6F_{14}, *Atmos. Chem. Phys.*, *12*, 11753–11764.

Dillon, T. J., A. Horowitz, and J. N. Crowley (2010), Cross-sections and quantum yields for the atmospheric photolysis of the potent greenhouse gas nitrogen trifluoride, *Atmos. Env.*, *44*(9), 1186–1191.

Dillon, T. J., L. Vereecken, A. Horowitz, V. Khamaganov, J. N. Crowley, and J. Lelieveld (2011), Removal of the potent greenhouse gas NF_3 by reactions with the atmospheric oxidants $O(^1D)$, OH and O_3, *Phys. Chem. Chem. Phys.*, *13*, 18600–18608.

Fleming, E. L., C. H. Jackman, D. K. Weisenstein, and M. K. W. Ko (2007), The impact of interannual variability on multidecadal total ozone simulations, *J. Geophys. Res.*, *112*, D10310.

Fleming, E. L., C. H. Jackman, R. S. Stolarski, and A. R. Douglas (2011), A model study of the impact of source gas changes on the stratosphere for 1850–2100, *Atmos. Chem. Phys.*, *11*, 8515–8541.

La Paglia, S. R., and A. B. F. Duncan (1961), Vacuum ultraviolet absorption spectrum and dipole moment of nitrogen trifluoride, *J. Chem. Phys.*, *34*, 1003–1007.

Makeev, G. N., V. F. Sinyanskii, and B. M. Smirnov (1975), Absorption spectra of certain fluorides in the near ultraviolet region, *Doklady Phys. Chem.*, *222*, 452–455.

Molina, L. T., P. J. Wooldridge, and M. J. Molina (1995), Atmospheric reactions and ultraviolet and infrared absorptivities of nitrogen trifluoride, *Geophys. Res. Lett.*, *22*.

Prather, M. J., and J. Hsu (2008), NF_3, the greenhouse gas missing from Kyoto, *Geophys. Res. Lett.*, *35*, L12810.

Rontu Carlon, N., D. K. Papanastasiou, E. L. Fleming, C. H. Jackman, P. A. Newman, and J. B. Burkholder (2010), UV absorption cross sections of nitrous oxide (N_2O) and carbon tetrachloride (CCl_4) between 210 and 350 K and the atmospheric implications, *Atmos. Chem. Phys.*, *10*, 6137–6149.

Sander, S. P., J. Abbatt, J. R. Barker, J. B. Burkholder, R. R. Friedl, D. M. Golden, R. E. Huie, C. E. Kolb, M. J. Kurylo, G. K. Moortgat, V. L. Orkin, and P. H. Wine, Jet Propulsion Laboratory, California Institute of Technology, Chemical Kinetics and Photochemical Data for Use in Atmospheric Studies, Evaluation Number 17, Pasadena, California, (2011).

Sorokin, V. I., N. P. Gristan, and A. I. Chichinin (1998), Collisions of $O(^1D)$ with HF, F_2, XeF_2, NF_3, and CF_4: Deactivation and reaction, *J. Chem. Phys.*, *108*, 8995–9003.

WMO (World Meteorological Organization) (2011), Scientific Assessment of Ozone Depletion: 2010, Global Ozone Research and Monitoring Project-Report No. 52, Geneva, Switzerland, 516 pp, Geneva, Switzerland.

Zhao, Z., P. L. Laine, J. M. Nicovich, and P. H. Wine (2010), Reactive and non-reactive quenching of $O(^1D)$ by the potent greenhouse gases SO_2F_2, NF_3, and SF_5CF_3, *Proc. Nat. Acd. Sci.*, *107*, 6610–6615.